Mechanics Research Communications 158 (2026) 104801

Contents lists available at ScienceDirect

Mechanics Research Communications

journal homepage: www.elsevier.com/locate/mechrescom

Supra-resonant wing oscillations in insect flight☆

G. Ferraro [a,1], D. Agostinelli [b,1], D. Romano [a,d], A. DeSimone [a,c,d,*]

[a] The Biorobotics Institute, Sant'Anna School of Advanced Studies, V.le R. Piaggio 34, Pontedera (PI), 56025, Italy
[b] DIISM, UNIVPM, Via Brecce Bianche, 12, Ancona, 60131, Italy
[c] MathLab, SISSA, Via Bonomea, 265, Trieste, 34136, Italy
[d] Department of Excellence in Robotics & A.I, Sant'Anna School of Advanced Studies, Pisa, 56127, Italy

ARTICLE INFO

Keywords:
Supra-resonant oscillations
Indirect insect flight
Hopf bifurcation
Limit cycle
Harmonic balance

ABSTRACT

We study a minimal dynamical model of the mechanism generating wing beats in insects based on a coupled wing–thorax–muscle oscillator with delayed muscle activation. The system exhibits self-sustained oscillations arising from an instability due to the stretch-activated muscle forcing. We identify two distinct dynamical regimes depending on the relative magnitude of the muscle response rate and the thoracic resonance frequency, corresponding to slow- and fast-muscle dynamics. In the slow-muscle regime, the instability is unconditional with respect to the muscle forcing and oscillations emerge at the natural mechanical frequency. In the fast-muscle regime, oscillations arise only above a finite threshold and are inherently supra-resonant already at their onset. Using the method of harmonic balance, we derive an analytical relation between oscillation amplitude and frequency that works beyond the weakly nonlinear regime. The analytical predictions are validated against numerical simulations, showing good agreement in the biologically relevant parameter range.

1. Introduction

Rhythmic oscillations are ubiquitous in both biological and engineered mechanical systems, mainly arising through two fundamentally distinct mechanisms: resonances associated with time-periodic external forcing, and spontaneous self-sustained oscillations emerging from internal instabilities. The latter mechanism, characterized by Hopf bifurcations and limit-cycle dynamics, underlies a surprisingly broad class of phenomena, from the beating of eukaryotic cilia [1,2] and the nutations in growing plant shoots [3–6], to the oscillatory dynamics of light-powered liquid crystal actuators [2,7,8].

A particularly striking biological realization of this principle is the indirect, asynchronous flapping flight of insects [9]. Unlike insects that activate their flight muscles synchronously with each wingbeat, as in the case of dragonflies [10–12], many species, including flies, bees, beetles, and mosquitoes, achieve wingbeat frequencies far beyond the bandwidth of direct neuromuscular control, exceeding 800 Hz in certain mosquito species [13]. In these insects, two antagonistic sets of muscles deform the thorax rather than acting directly on the wings, and the wingbeat frequency emerges not from neural firing rates, but from an oscillatory instability of the coupled muscle–thorax–wing system [9]. This indirect flight mechanism constitutes one of the major evolutionary innovations in animal locomotion, enabling small insects to generate sufficient aerodynamic lift despite their limited wing area, and is widely credited with driving the extraordinary species radiation observed in these groups [14]. This mechanism has also inspired artificial robotic systems that mimic insect flight, such as the centimeter-scale robots RoboBee [15,16] and Bee+ [17].

Prior studies have examined this mechanism primarily through numerical simulations within the specific context of insect thorax mechanics [9,18], establishing that wingbeats arise as a Hopf bifurcation phenomenon. However, the precise dynamical origin of the emergent supra-resonant wingbeats remains unresolved: it is unclear whether supra-resonancy arises directly at the onset of the bifurcation — implying that active muscle kinetics alter the natural frequency of the passive system, as seen in other physical models exhibiting analogous instabilities [2] - or whether it is a post-bifurcation consequence of operating far from the instability threshold. Moreover, it has not yet been attempted to analytically predict the oscillation frequency and amplitude within the biologically relevant parameter domain.

In this work, we address these questions by providing a systematic mathematical analysis of the simplified model for insects wing-beat dynamics presented in [9]. We begin by identifying two qualitatively distinct Hopf bifurcation scenarios. In the regime where the muscle response is slow relative to the mechanical resonance timescale, the

☆ This article is part of a Special issue entitled: 'Multiscale Metamaterials' published in Mechanics Research Communications.

* Corresponding author at: The Biorobotics Institute, Sant'Anna School of Advanced Studies, V.le R. Piaggio 34, Pontedera (PI), 56025, Italy.
E-mail addresses: desimone@sissa.it, a.desimone@santannapisa.it (A. DeSimone).

[1] Equal contribution.

https://doi.org/10.1016/j.mechrescom.2026.104801
Received 30 June 2026; Received in revised form 30 July 2026; Accepted 13 August 2026
Available online 31 August 2026
0093-6413/© 2026 The Authors. Published by Elsevier Ltd. This is an open access article under the CC BY-NC-ND license (http://creativecommons.org/licenses/by-nc-nd/4.0/).

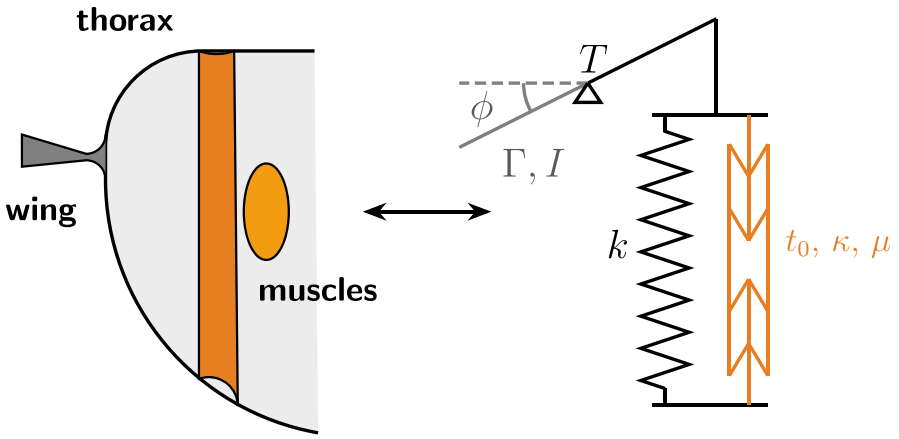


Fig. 1. Schematic of the insect muscle-thorax–wing system (left) and its corresponding mechanical model (right). The system is modeled via Eq. (1) as a spring–mass–damper oscillator governing the wing angle ϕ. The linear thoracic stiffness k and the muscle force act in parallel on the wing through a rigid hinge with transmission ratio T. The wing is characterized by an effective moment of inertia I (including added air mass) and is subject to a quadratic aerodynamic damping coefficient Γ. The muscle force is governed by the stretch-activation kinetics described by Eq. (2) and parameterized by the characteristic delay t_0, the relaxation-to-contraction rate ratio κ, and the feedback scaling amplitude μ.

instability gives rise to limit-cycle oscillations at the passive mechanical resonance frequency. In the opposite limit, where the muscle dynamics are fast, the bifurcation occurs at a frequency exceeding the mechanical resonance, characteristic of the supra-resonant regime. We further situate these two regimes within the broader landscape of oscillatory dynamical systems by drawing explicit comparisons with other physical and biological systems exhibiting analogous instabilities, elucidating both the structural analogies and the fundamental distinctions. We note that, among the few insect species for which the relevant muscle parameters have been experimentally measured, all appear to lie within the slow-muscle regime, whereas no known species has yet been identified in the fast-muscle regime. Nevertheless, the bifurcation structure associated with the latter shares important similarities with that of other oscillatory systems and could provide useful insights for the design of bio-inspired artificial devices.

To obtain analytical predictions valid beyond the weakly nonlinear approximation, we employ the method of harmonic balance, from which we derive a closed-form relationship between oscillation amplitude and frequency. This expression remains accurate well into the strongly nonlinear regime, far from the bifurcation point, where standard normal-form reductions are no longer applicable. The analytical results are validated against numerical simulations of the full governing equations, demonstrating that the derived expressions correctly reproduce the qualitative behavior and yield quantitative agreement across the biologically relevant parameter range.

The rest of the paper is organized as follows. In Section 2.1, we present the governing equations of the muscle–thorax–wing system introduced in [9]. In Section 2.2, we perform a linear stability analysis of the trivial equilibrium using the Routh–Hurwitz criterion, showing that the system can undergo a Hopf bifurcation. In Section 2.3, we characterize the two qualitatively distinct bifurcation regimes that arise depending on the relative magnitude of the muscle activation timescale and the mechanical resonance period. In Section 2.4, we employ the method of harmonic balance to derive closed-form analytical expressions for the oscillation frequency and amplitude valid in the strongly nonlinear regime. Finally, in Section 2.5, we validate the analytical expressions for the amplitude and frequency with the numerical solutions within the biologically relevant domain.

2. Model, analysis, and results

2.1. Mathematical model

Following previous studies [18], we model the muscle–thorax–wing system of an asynchronous flying insect as two coupled second-order differential equations:

$$\ddot{\phi} + \beta_1 \dot{\phi}|\dot{\phi}| + \beta_0 \phi = cf, \tag{1}$$

$$\dot{f} + \alpha_2 f + \alpha_3 f = -\alpha_3 \dot{\phi}, \tag{2}$$

where ϕ is the wing angle relative to the horizontal plane, f represents the muscle-generated force (Fig. 1), and the overdots $\dot{()}$ denote time differentiation.

Eq. (1) is an effective second-order oscillator that describes the wing motion. It accounts for inertia ($\ddot{\phi}$), aerodynamic drag as a quadratic viscous term ($\beta_1 \dot{\phi}|\dot{\phi}|$) [19], elasticity of the thorax and muscles as a linear elastic term ($\beta_0 \phi$), and muscle-generated torque through a coupling term (cf). In particular, the structural parameters are defined as

$$\beta_1 = \frac{\Gamma}{I}, \qquad \beta_0 = \frac{k}{IT^2}, \qquad c = \frac{\mu}{IT}, \tag{3}$$

where Γ is the aerodynamic damping coefficient, T is the wing hinge transmission ratio (the ratio of angular wing displacement to muscle displacement), I is the combined inertia of the wings and the added mass of air, k is the linear thorax stiffness, and μ scales the muscle forcing strength (Fig. 1). In the absence of muscle coupling ($c = 0$) and aerodynamic damping ($\beta_1 = 0$), the parameter β_0 defines the squared natural frequency of the passive (undamped) system, i. e.,

$$\omega_n := \sqrt{\beta_0}. \tag{4}$$

Eq. (2) provides a phenomenological model of the mechanical feedback behavior characteristic of asynchronous flight muscles [9,20]. In contrast to synchronous flight, which requires an individual neural impulse for each wingstroke, asynchronous systems rely on muscles that remain continuously active under a baseline neural firing rate. Instead of direct neural pacing, rhythmic contractions are driven mechanically by two complementary processes: delayed stretch activation (dSA) and delayed shortening deactivation (dSD) [21]. To capture this time-dependent mechanical response, Eq. (2) acts as a second-order linear filter driven by the kinematic strain rate $\dot{\phi}$. Consequently, a mechanical stretch results in a force profile that peaks and relaxes after a characteristic time delay, providing the necessary phase lag to inject energy into the wingbeat cycle. The filter coefficients are defined as

$$\alpha_2 = \frac{\ln(1/\kappa)(1+\kappa)}{t_0(1-\kappa)}, \qquad \alpha_3 = \frac{\kappa \ln^2(1/\kappa)}{t_0^2(1-\kappa)^2}, \tag{5}$$

where the parameters t_0 and κ are determined by fitting experimental muscle response data [9,20]. Specifically, t_0 is the temporal delay

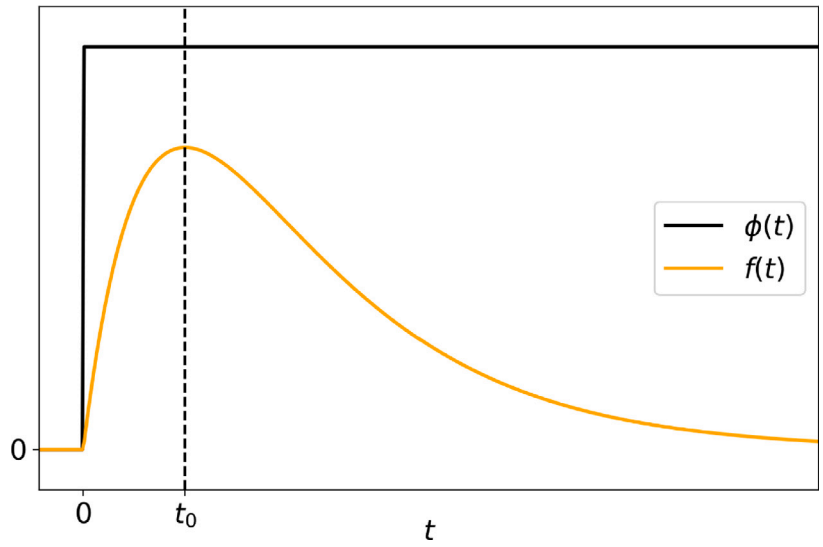


Fig. 2. Force response $f(t)$ to an externally imposed step-like angular displacement, obtained by solving Eq. (2). The response reaches a maximum proportional to μ at time t_0, after which it decays to zero for long times [9].

Table 1
Choice of model parameters for the numerical solutions [9].

Parameter	Description	Value
I	Wing inertia	6.8×10^{-11} kg m^2
Γ	Aerodynamic damping parameter	1.1×10^{-11} kg m^2
k	Linear thorax stiffness	6.4×10^{3} N m^{-1}
T	Wing hinge transmission ratio	1.5×10^{4} m^{-1}
t_0	Muscle activation delay	4.4×10^{-3} s (slow-muscle) 1.0×10^{-3} s (fast-muscle)
κ	Muscle rate ratio	1.7×10^{-1}

between the external stretch and the peak muscle force, and κ is the ratio between the muscle relaxation and contraction rates (Fig. 2).

System (1)–(2) has been proposed in [9] to study insect flapping flight driven by asynchronous muscles, with the aim of characterizing the wingbeat as an emergent feature arising from the mechanical instabilities of the coupled muscle–thorax–wing system. Although this formulation effectively captures the primary oscillatory dynamics, more sophisticated kinematic and aerodynamic models are necessary to resolve other interesting details of insect flight, such as wing rotation and figure-eight trajectories of the wing tips, leading and trailing edge vortices, and wake capture phenomena. Indeed, a single-angle kinematic description like Eq. (1) enforces a reciprocal trajectory (where the upstroke retraces the downstroke in reverse), and the local quadratic damping term simplifies the highly non-local, unsteady fluid mechanics inherent to flapping flight [22].

System (1)–(2) admits the trivial equilibrium $(\phi, f) = (0, 0)$, which corresponds to the wing at rest. The stability of this equilibrium depends on the system parameters and, in particular, on the muscle coupling coefficient c. When c exceeds a critical threshold, the equilibrium becomes unstable, giving rise to self-sustained wingbeats, with the nonlinear aerodynamic drag $\beta_1\dot\phi|\dot\phi|$ acting as a stabilizing mechanism. The amplitude and frequency of the emerging oscillations are determined by the interplay between the linear instability and the nonlinear damping.

2.2. Linear stability and bifurcation analysis

To study the stability of the trivial equilibrium $(\phi, f) = (0, 0)$, we linearize the system (1)–(2). By substituting f from the linearized version of Eq. (1) into Eq. (2), we reduce the linearized system to an equivalent single fourth-order linear differential equation in terms of the wing angle ϕ, i.e.,

$$\ddddot\phi + \alpha_2\dddot\phi + (\beta_0+\alpha_3)\,\ddot\phi + (\alpha_2\beta_0 + c\alpha_3)\,\dot\phi + \alpha_3\beta_0\,\phi = 0. \tag{6}$$

The corresponding characteristic equation is given by

$$\lambda^4 + a_3\lambda^3 + a_2\lambda^2 + a_1\lambda + a_0 = 0, \tag{7}$$

where the polynomial coefficients map directly to the physical parameters of Eq. (6) as $a_3 = \alpha_2$, $a_2 = \beta_0 + \alpha_3$, $a_1 = \alpha_2\beta_0 + c\alpha_3$, and $a_0 = \alpha_3\beta_0$.

The trivial equilibrium is asymptotically stable if and only if all roots of the characteristic polynomial have strictly negative real parts. According to the Routh–Hurwitz criterion, this is verified if and only if

$$a_i > 0 \ \ \forall i, \qquad a_3a_2 > a_1, \qquad a_3a_2a_1 > a_1^2 + a_3^2a_0. \tag{8}$$

Since the parameters α_2, α_3, and β_0 are strictly positive in biological systems [9], the inequalities (8) reduce to

$$c\,(\alpha_2\alpha_3 - c\alpha_3 - \beta_0\alpha_2) > 0. \tag{9}$$

The quadratic inequality (9) in terms of the coupling parameter c yields the stability condition

$$\begin{cases} c_{\text{crit}} < c < 0, & \text{if } \alpha_3 < \beta_0, \\ 0 < c < c_{\text{crit}}, & \text{if } \alpha_3 > \beta_0, \end{cases} \qquad \text{where} \quad c_{\text{crit}} := \alpha_2\left(1 - \frac{\beta_0}{\alpha_3}\right). \tag{10}$$

From a biological perspective, the coupling coefficient c must be non-negative because muscles can only generate tensile (pulling) forces. Consequently, the system dynamics is completely determined by the relative timescales of the structural resonance (β_0) and the muscle-feedback activation ($\alpha_3 \propto 1/t_0^2$).

In the fast-muscle regime, where the muscle feedback is faster than the structural resonance frequency ($\alpha_3 > \beta_0$), the critical threshold c_{crit} is strictly positive so that the system remains stable for weak muscle coupling ($0 < c < c_{\text{crit}}$). Instead, in the slow-muscle regime ($\alpha_3 < \beta_0$), the trivial equilibrium becomes unstable for any positive coupling strength ($c > 0$), meaning the system initiates flapping as soon as muscle activity is present, without requiring a minimum activation threshold.

The transition from a stable steady state to self-sustained oscillations occurs via a Hopf bifurcation when a pair of complex conjugate eigenvalues crosses the imaginary axis (Fig. 3). Substituting $\lambda = i\omega$ into

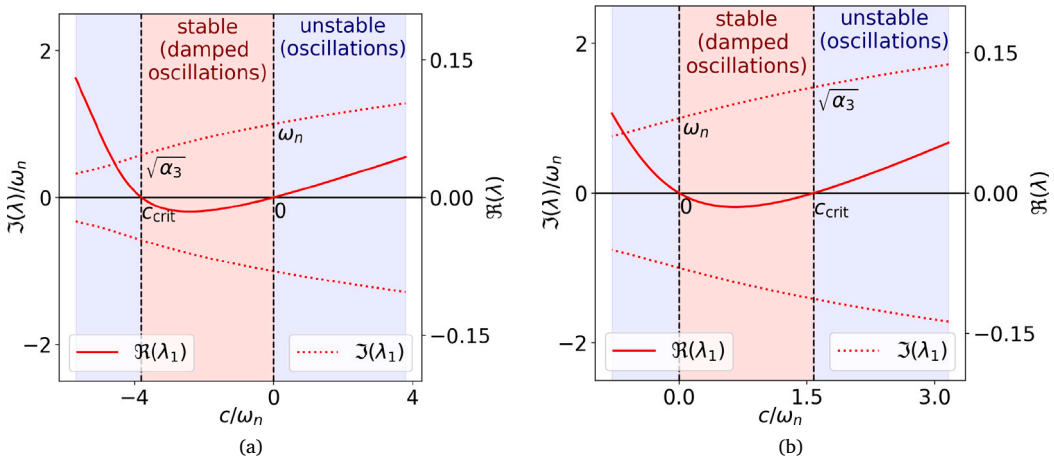


Fig. 3. Bifurcation diagrams showing the real (solid lines) and imaginary (dashed lines) parts of the leading eigenvalues of the characteristic Eq. (7) as a function of the muscle coupling parameter c, for the choice of model parameters as in Table 1. Red and blue backgrounds denote stable (damped oscillations, $\Re(\lambda) < 0$) and unstable (growing oscillations, $\Re(\lambda) > 0$) regions, respectively. (a) Slow-muscle regime ($\sqrt{\alpha_3} < \omega_n$): the system is unstable for any active coupling ($c > 0$), undergoing a Hopf bifurcation at $c = 0$ with an emergent frequency equal to the passive structural resonance, $\omega_H = \omega_n$. (b) Fast-muscle regime ($\sqrt{\alpha_3} > \omega_n$): the equilibrium remains stable until c reaches the critical threshold $c_{\text{crit}} > 0$, where a Hopf bifurcation yields a dynamic wingbeat frequency governed by the active muscle kinetics, $\omega_H = \sqrt{\alpha_3} > \omega_n$.

the characteristic Eq. (7) and solving for ω, we determine the onset oscillation frequency as a function of the active coupling, i.e.,

$$\omega_H^2 = \frac{\alpha_2\beta_0 + c\alpha_3}{\alpha_2}. \tag{11}$$

Evaluating this expression reveals a direct link to the underlying timescales of the system. In the slow-muscle regime, the Hopf bifurcation at $c = 0$ produces oscillations at the natural frequency of the passive, undamped thorax–wing system, $\omega_H = \omega_n = \sqrt{\beta_0}$ (Fig. 3(a)). In the fast-muscle regime, the bifurcation at $c = c_{\text{crit}}$ results into wingbeats at a supra-resonant frequency $\omega_H = \sqrt{\alpha_3} > \omega_n$, governed by the intrinsic activation rate of the muscle (Fig. 3(b)).

2.3. The bifurcation in terms of the stretch-activation delay t_0

The preceding analysis characterizes the stability of the system in terms of the muscle activation intensity c. However, from a physiological point of view, a more natural control parameter is the stretch-activation delay t_0, which controls the internal timescale of the asynchronous muscle response. Using Eq. (5), we rewrite the stability condition (9) as a quadratic inequality in terms of t_0, yielding the critical delay threshold

$$t_0^\star := \frac{2\kappa\ln(1/\kappa)}{\kappa c + \sqrt{(\kappa c)^2 + 4\kappa(1-\kappa)^2\omega_n^2}}, \tag{12}$$

below which the trivial equilibrium remains stable.

To contextualize this critical threshold within the previously defined "fast" and "slow" muscle regimes, we introduce a secondary characteristic timescale corresponding to the condition $\alpha_3 = \beta_0$, i.e.,

$$t_0^{\star\star} := \frac{1}{\omega_n}\frac{\sqrt{\kappa}\ln(1/\kappa)}{1-\kappa}, \tag{13}$$

so that the muscle frequency is equal to the natural one for $t_0 = t_0^{\star\star}$. Since $t_0^\star(c)$ is a strictly decreasing function of the active coupling c and $t_0^\star(c = 0) = t_0^{\star\star}$, it follows that $t_0^\star < t_0^{\star\star}$ for any biological active system ($c > 0$). Therefore, in terms of the insect stretch-activation delay t_0, we can distinguish three distinct operational regimes that clarify the nature of emergent supra-resonant wingbeats (Fig. 4).

1. The stable ultra-fast regime ($0 < t_0 < t_0^\star$), where the muscle responds so rapidly to mechanical strain that the phase lag between elongation and active force generation is insufficient to inject net energy into the system. The critical activation threshold required to destabilize the equilibrium exceeds the actual muscle strength ($c < c_{\text{crit}}$), preventing the emergence of spontaneous oscillations.
2. The conditionally active fast regime ($t_0^\star < t_0 < t_0^{\star\star}$), where the muscle operates faster than the structural resonance ($\alpha_3 > \beta_0$), but its delay is long enough that the muscle coupling can overcome passive damping ($c > c_{\text{crit}} > 0$). At the bifurcation threshold, the wing oscillates at an active, supra-resonant frequency ($\omega_H = \sqrt{\alpha_3} > \omega_n$). In this regime, supra-resonancy arises because the muscle activity modulates the structural mechanics - a mechanism analogous to the elastic-inertial and negative-damping feedbacks observed in active planar filaments, such as eukaryotic cilia and photo-responsive liquid crystal elastomer rods [2].
3. The unconditionally unstable slow-muscle regime ($t_0 > t_0^{\star\star}$), where the stretch-activation delay is long enough that the muscle feedback is inherently slower than the structural resonance ($\alpha_3 < \beta_0$). This forces the critical threshold to zero ($c_{\text{crit}} < 0$), meaning that any positive muscle coupling ($c > 0$) destabilizes the steady state and guarantees spontaneous flapping.

Comparing the actual values of t_0 against the thresholds $t_0^\star$ and $t_0^{\star\star}$ for *Bombus impatiens* and *Drosophila melanogaster*, we find that both insects reside within the slow-muscle regime (Table 2, [9]). Therefore, the underlying Hopf bifurcation occurs precisely at $c = 0$, where the onset frequency matches the passive mechanical resonance ($\omega_H = \omega_n$). However, since insects (such as *Bombus* and *Drosophila* [9]) operate at a finite, strictly positive muscle strength ($c > 0$), their wingbeats fall within the unstable post-bifurcation domain. As the system moves further past the bifurcation point, nonlinear interactions pull the operational frequency upward (Fig. 3). In this slow-muscle regime, the observed supra-resonant wingbeat is not a manifestation of an altered threshold frequency (as seen in the cilia-like behavior of the second regime), but rather a nonlinear consequence of operating beyond a structural instability.

2.4. Nonlinear limit cycle analysis and the infinite muscle-delay limit

To approximate the amplitude and frequency of the emerging limit cycle, we use the first-order harmonic balance method [23]. Assuming

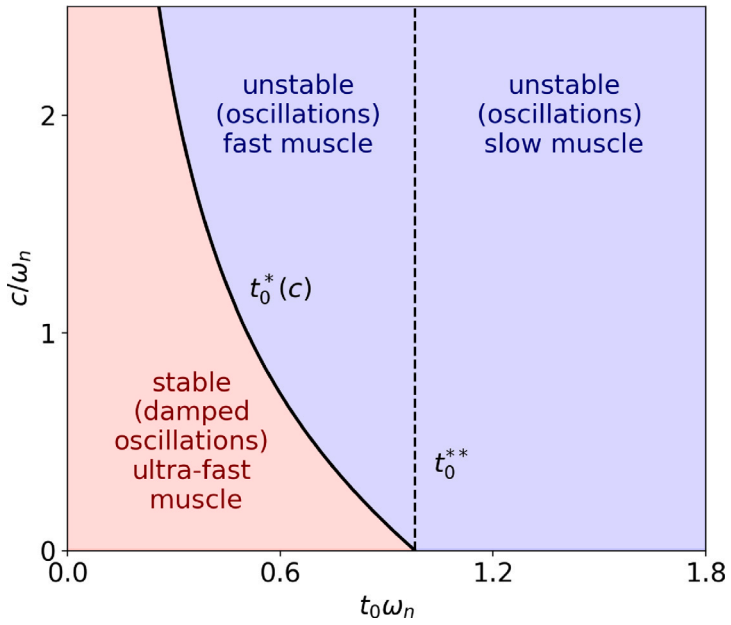


Fig. 4. Diagram illustrating the three operational regimes of the muscle–thorax–wing system as a function of the stretch-activation delay t_0 and the muscle coupling coefficient c. The system transitions from a stable state of damped oscillations to conditional active flapping at $t_0 = t_0^\star(c)$, and finally enters an unconditionally unstable flapping regime once the delay exceeds the passive structural timescale $t_0^{\star\star}$.

Table 2
Critical parameters for *Bombus impatiens* (bumblebee) and *Drosophila melanogaster*, evaluated from the measured values of ω_n and κ in [9]. Both species satisfy $t_0 > t_0^{**}$, placing them in the slow-muscle regime, where the Hopf bifurcation occurs at $c = 0$ and supra-resonant wingbeats emerge as a nonlinear consequence of operating beyond the instability threshold.

Species	t_0	κ	t_0^{**}
Bombus impatiens	4.4 ms	0.17	1.4 ms
Drosophila melanogaster	6.7 ms	0.02	0.5 ms

a fundamental harmonic solution of the form $\phi(t) = A\cos(\omega t)$, we approximate the non-smooth quadratic damping term by a first-order Fourier expansion, namely

$$\beta_1|\dot\phi|\dot\phi \approx \tilde\beta_1\dot\phi, \qquad \text{where} \quad \tilde\beta_1 = \frac{8}{3\pi}\beta_1 A\omega. \tag{14}$$

Substituting this linear damping into Eqs. (1)–(2), we get a single, linear fourth-order equation in the time domain

$$\dddot\phi + (\tilde\beta_1+\alpha_2)\ddot\phi + (\beta_0+\alpha_2\tilde\beta_1+\alpha_3)\dot\phi + (\alpha_2\beta_0+\alpha_3\tilde\beta_1+c\alpha_3)\phi + \alpha_3\beta_0\phi = 0. \tag{15}$$

Balancing the terms proportional to $\cos(\omega t)$ and $\sin(\omega t)$ yields the algebraic conditions that govern the steady-state limit cycle. Treating ω as an independent parameter, we obtain explicit expressions for the bifurcation parameter c and the response amplitude A as functions of the oscillation frequency ω, namely,

$$c(\omega) = \frac{(\omega^2-\beta_0)}{\alpha_2\alpha_3}\left[\alpha_2^2 + \frac{(\alpha_3-\omega^2)^2}{\omega^2}\right], \tag{16}$$

$$A(\omega) = \frac{3\pi\,(\beta_0-\omega^2)\,(\alpha_3-\omega^2)}{8\beta_1\alpha_2\omega^3}. \tag{17}$$

Although Cardano's formula can yield explicit expressions for ω and A, the closed-form representation above suffices to explore limit regimes and trace the amplitude and frequency of emerging oscillations as functions of the bifurcation parameter c (Fig. 5). Notably, a local asymptotic expansion of Eqs. (16)–(17) near either bifurcation threshold ($c \to 0$ or $c \to c_{\text{crit}}$) reveals that the steady-state amplitude scales linearly with the control parameter (i.e., $A \propto |c - c_{\text{crit}}|$ or $A \propto |c|$). This linear scaling is a distinct signature of the quadratic aerodynamic drag, representing a fundamental difference from classic systems with cubic nonlinearities, such as the Van der Pol oscillator, where the amplitude typically scales with the square root of the bifurcation parameter.

Finally, we test the behavior of the system in the limit of an infinitely long muscle delay. Using Eq. (5), we rewrite Eq. (16) as

$$(\omega_n^2-\omega^2)\left[\frac{C_2^2}{t_0^2}\,\omega^2 + \left(\frac{C_3}{t_0^2}-\omega^2\right)^2\right] + c\,\frac{C_3\,C_2}{t_0^3}\,\omega^2 = 0, \tag{18}$$

where $C_2 = \ln(1/\kappa)(1+\kappa)/(1-\kappa)$ and $C_3 = \kappa\left[\ln(1/\kappa)/(1-\kappa)\right]^2$. As the stretch-activation delay becomes infinitely long ($t_0 \to \infty$), all terms in Eq. (18) scaled by inverse powers of t_0 vanish, yielding

$$(\omega_n^2-\omega^2)\,\omega^4 = 0. \tag{19}$$

Since a valid limit cycle requires a non-vanishing frequency ($\omega \neq 0$), the unique stable solution for the emergent oscillation frequency is

$$\omega = \omega_n. \tag{20}$$

Thus, for increasing values of t_0, muscle dynamics becomes slower and the oscillation frequency converges to the undamped mechanical resonant frequency of the wing–thorax system, ω_n, in agreement with the results in [9].

2.5. Numerical results

To validate our analytical predictions, we implement numerically the nonlinear coupled system (1)–(2), by recasting it as a first-order dynamical system by introducing the auxiliary variables $\psi = \dot\phi$ and $F = \dot f$:

$$\dot\phi = \psi, \tag{21}$$

$$\dot\psi = -\beta_1\psi|\psi| - \beta_0\phi + c\,f, \tag{22}$$

$$\dot f = F, \tag{23}$$

$$\dot F = -\alpha_2 F - \alpha_3 f - \alpha_3\psi. \tag{24}$$

We integrate this four-dimensional system using the explicit Runge–Kutta method of order 5(4) (RK45), using the function `integrate.solve_ivp` of the SciPy package [24]. We apply a perturbation to

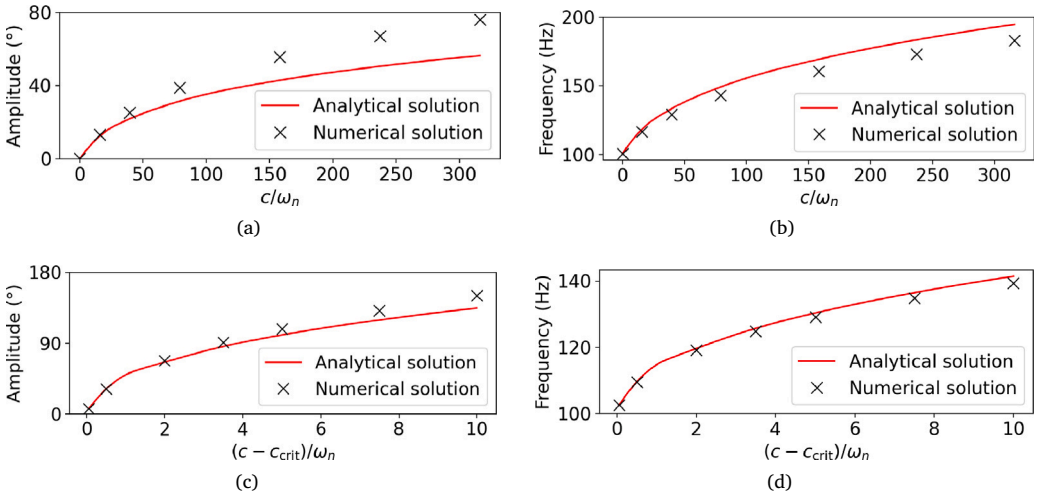


Fig. 5. Comparison of wingbeat amplitude (a,c) and frequency (b,d) between the analytical expressions, Eqs. (16)–(17), and numerical solutions of system (21)—(24), with the parameters listed in Table 1. Panels (a,b) are for the slow-muscle regime ($\alpha_3 < \beta_0$) and (c,d) for the fast-muscle regime ($\alpha_3 > \beta_0$). The comparison is reported for biologically relevant values of the oscillation frequency (100–200 Hz) and amplitude (70°–150°).

the trivial equilibrium by imposing the initial condition $(\phi, \psi, f, F) = (\delta\phi, 0, 0, 0)$ and we evaluate the frequency and amplitude of the emergent oscillations after the initial transient response.

Fig. 5 shows the comparison between numerical results and analytical expressions given by Eqs. (16)–(17). To verify numerical convergence, we reduced the integration tolerances of the adaptive solver by an order of magnitude; the resulting steady-state metrics shifted by less than 1%, confirming that numerical truncation errors are negligible.

Numerical simulations are in agreement with the analytical results in both regimes, despite discrepancies introduced by the first-order harmonic approximation. In particular, the predictions for the oscillation frequency (Figs. 5(b), 5(d)) are more accurate than those for the amplitude (Figs. 5(a), 5(c)) which exhibit errors on the order of 20% far from the bifurcation point, while still capturing the correct qualitative behavior.

3. Discussion

The dynamical framework considered here is based on the reduced-order biophysical model introduced by Wold et al. [9], which capture the essential mechanical feedback mechanisms underlying asynchronous insect flight. In particular, the model incorporates experimentally informed estimates of thoracic stiffness, muscle activation times, and mechanical resonance properties, providing a minimal representation of the coupled muscle–thorax–wing dynamics. While the biological motivation and parameter selection originate from these previous studies, the present work focuses on a systematic characterization of the nonlinear dynamical mechanisms governing the emergence and evolution of self-sustained oscillations.

The linear stability analysis presented in Section 2.3 reveals that the onset of oscillatory instability can occur in two qualitatively distinct regimes, depending on whether the intrinsic muscle timescale t_0 is long or short relative to the mechanical resonance period $2\pi/\omega_n$.

In the slow-muscle regime ($\alpha_3 < \beta_0$), the instability is unconditional with respect to the control parameter c; the rest state becomes unstable for any positive value of c, and the bifurcation frequency coincides with the mechanical resonance frequency ω_n. As shown in Fig. 5, both the oscillation frequency and the amplitude increase monotonically with c beyond the bifurcation point. Consequently, supra-resonant behavior is achieved only by actively tuning the muscle response strength, rather than being present already at the onset of the bifurcation. This regime is therefore characterized by a smooth, robust transition to large-amplitude, supra-resonant oscillations driven by the nonlinear dynamics of the system.

In the fast-muscle regime ($\alpha_3 > \beta_0$), by contrast, the instability requires the control parameter to exceed a finite threshold $c > c_{crit} > 0$, and the bifurcation frequency is $\sqrt{\alpha_3} > \omega_n$, meaning that the system is already supra-resonant at onset. This phenomenology is structurally analogous to that observed in other spontaneously oscillating biological systems, such as eukaryotic cilia and photo-deformable liquid crystal elastomer rods [2], where the oscillation frequency at bifurcation is determined by internal dynamical timescales rather than by mechanical resonance.

Experimental data for asynchronous insects, including *Bombus* (bumblebees) and *Drosophila*, for which the parameters α_3 and β_0 have been estimated in [9], indicate that these species operate in the slow-muscle regime. Their stretch-activation timescales ($t_0 \approx 4$–$7\,\mathrm{ms}$) are sufficiently long relative to their thoracic mechanical resonance period ($f_n := \omega_n/(2\pi) > 100\,\mathrm{Hz}$) that the condition $t_0 > t_0^{\star\star}$ is satisfied. From a functional perspective, operating in this regime may confer a significant robustness advantage: since the instability is unconditional in c, the transition to sustained oscillations does not require precise tuning of the neural drive. Any baseline level of tetanic stimulation is sufficient to destabilize the rest state, and supra-resonant limit-cycle oscillations emerge through a robust, self-sustaining mechanism. This insensitivity to fine-tuning of the control parameter may represent an evolutionary advantage, reducing the precision demands on the neuromuscular control system, hence enabling the system to maintain steady flapping even in the presence of physiological (e.g., aging) or environmental (e.g., temperature) variability. Moreover, the decoupling between the mechanisms of lift generation (through fast wingbeats) and control for maneuvering (that is obtained by the action of steering muscles without changing the frequency of the wingbeat), that is characteristic of indirect flight, may also be interpreted in terms of evolutionary advantages with respect to direct flight, where the frequency of the beat of each wing is controlled individually by a dedicated muscle.

To the best of our knowledge, no experimental evidence has been reported yet for insects operating in the fast-muscle regime. Parameters t_0 and κ have been quantified in only a limited number of species, all of which fall within the slow-muscle regime. It would be interesting to know whether there are fundamental reasons that force biological systems in this regime, or if there are instead exceptions. In addition, extending this analysis to other insect orders and species would clarify whether the two muscle regimes, fast and slow, may reflect different

evolution trajectories in asynchronous flight, and not just physiological differences between species of the same order.

Moving from biology to robotics, the fast-muscle regime that we have identified may be of relevance for bio-inspired artificial systems, where actuation timescales and control architectures can differ substantially from those of biological organisms, and where supra-resonant oscillations at the onset of the bifurcation may be desirable for engineering applications. Here, our results could pave the way to design criteria to tune actuator dynamics and structural resonance in flapping robots, thereby achieving the desired combination of robustness, energetic optimality, and maneuverability.

Beyond the linear stability analysis, we derived an analytical expression for the oscillation amplitude and frequency in the nonlinear regime using the method of harmonic balance. This approach yields closed-form predictions that remain valid well beyond the weakly nonlinear approximation and are in good quantitative agreement with numerical solutions across the biologically relevant parameter range.

We note that all the results obtained in this work should be interpreted as properties of the specific reduced-order model considered here. Therefore, the extent to which these conclusions can be generalized to real insect flight remains to be assessed by future studies. In particular, the present formulation assumes linearized thorax mechanics and does not account for geometric or material nonlinearities in the thoracic structure or in the wing transmission mechanism. Additionally, the model does not account for aerodynamic feedback or active control muscles, used by insects to modulate wing kinematics. These may influence both the oscillation amplitude and the effective nonlinear response of the system. Incorporating these effects represents a natural direction for future theoretical and experimental work.

4. Conclusions

We have presented a detailed mathematical study of the minimal model for indirect insect flight presented in [9] and that was previously analyzed primarily through numerical simulations. According to this model, oscillations emerge from a Hopf bifurcation in a coupled muscle–thorax–wing system. The analysis reveals the existence of two qualitatively distinct dynamical regimes, governed by the relative timescales of muscle activation and mechanical resonance. In the slow-muscle regime, the bifurcation occurs at the mechanical resonance frequency, and large-amplitude oscillations are achieved by driving the system deep into the nonlinear regime by increasing the muscle forcing strength. In the fast-muscle regime, by contrast, the instability gives rise to supra-resonant oscillations already at the bifurcation point, with the oscillation frequency determined by the interplay between muscle dynamics and mechanical response. To obtain quantitative predictions valid beyond the weakly nonlinear approximation, we employed the method of harmonic balance and derived a closed-form analytical relationship between the oscillation amplitude and frequency. This expression remains accurate well into the strongly nonlinear regime and yields good quantitative agreement with numerical solutions of the full governing equations across the biologically relevant parameter range. Comparison with experimental data suggests that insects operate predominantly in the slow-muscle regime, consistent with the observed robustness of resonance-frequency oscillations near onset. Whether this operating point reflects physiological constraints on muscle response times and thoracic mechanical properties, or whether it confers an evolutionary advantage through reduced sensitivity to fine-tuning of the control parameter, remains an open question. In fact, this sensitivity may be turned into an asset for the maneuverability of robotic insects. Future systematic measurements of the muscle activation timescale t_0 and the structural frequency ω_n in a broader range of species could help discriminate between these hypotheses and further test the validity of the proposed dynamical classification.

Future work will focus on incorporating more detailed muscle models, three-dimensional wing kinematics, and non-local aerodynamic feedback mechanisms to assess the robustness and generality of the reduced-order model considered here. Such extensions will help establish whether increasing the model fidelity primarily leads to quantitative refinements of the predicted dynamics or whether it also gives rise to qualitative changes in the bifurcation structure and the resulting oscillatory regimes.

CRediT authorship contribution statement

G. Ferraro: Writing – review & editing, Writing – original draft, Software, Methodology, Investigation, Formal analysis, Conceptualization. **D. Agostinelli:** Writing – review & editing, Writing – original draft, Methodology, Investigation, Formal analysis, Conceptualization. **D. Romano:** Writing – review & editing, Validation, Conceptualization. **A. DeSimone:** Writing – review & editing, Writing – original draft, Validation, Supervision, Project administration, Investigation, Funding acquisition, Conceptualization.

Acknowledgments

This work was inspired by prof. S. Sponberg's seminar 'Supra-resonant dynamics and self-excited oscillations in insect and robot flight', held on February 26th 2026 as part of the series on 'The mathematical laws of morphology and biomechanics' organized by K.L. Foster and A.M. Selvitella. Part of this research was carried out in the framework of the EU HORIZON PATHFINDEROPEN Project 'SENSORBEES – Sensorbees are ENhanced Self-ORganizing Bio-hybrids for Ecological and Environmental Surveillance' [GA 101130325].

Declaration of competing interest

The authors declare that they have no known competing financial interests or personal relationships that could have appeared to influence the work reported in this paper.

Data availability

Data will be made available on request.

References

[1] Irene Anello, François Alouges, Antonio De Simone, Beating of eukaryotic flagella via Hopf bifurcation of a system of stalled molecular motors, Eur. J. Mech. A Solids (ISSN: 09977538) 114 (2025) 105729, http://dx.doi.org/10.1016/j.euromechsol.2025.105729.

[2] Daniele Agostinelli, Irene Anello, Reza Norouzikudiani, Antonio DeSimone, Spontaneous oscillations in eukaryotic cilia and photo-responsive rods, J. Mech. Phys. Solids (ISSN: 00225096) 210 (2026) 106529, http://dx.doi.org/10.1016/j.jmps.2026.106529.

[3] Derek E. Moulton, Hadrien Oliveri, Alain Goriely, Multiscale integration of environmental stimuli in plant tropism produces complex behaviors, Proc. Natl. Acad. Sci. 117 (51) (2020) 32226–32237.

[4] Daniele Agostinelli, Alessandro Lucantonio, Giovanni Noselli, Antonio DeSimone, Nutations in growing plant shoots: The role of elastic deformations due to gravity loading, J. Mech. Phys. Solids (ISSN: 00225096) 136 (2020) 103702, http://dx.doi.org/10.1016/j.jmps.2019.103702.

[5] D. Agostinelli, A. DeSimone, G. Noselli, Nutations in plant shoots: Endogenous and exogenous factors in the presence of mechanical deformations, Front. Plant Sci. (ISSN: 1664-462X) 12 (2021) 371, http://dx.doi.org/10.3389/fpls.2021.608005, URL https://www.frontiersin.org/article/10.3389/fpls.2021.608005.

[6] D. Agostinelli, G. Noselli, A. DeSimone, Nutations in growing plant shoots as a morphoelastic flutter instability, Philos. Trans. R. Soc. A: Math. Phys. Eng. Sci. 379 (2201) (2021) 20200116, http://dx.doi.org/10.1098/rsta.2020.0116, URL https://royalsocietypublishing.org/doi/abs/10.1098/rsta.2020.0116.

[7] Reza Norouzikudiani, Luciano Teresi, Antonio DeSimone, Self-oscillations of submerged liquid crystal elastomer beams driven by light and self-shadowing, J. Elasticity 156 (4) (2024) 1243–1260.

[8] Alain Goriely, Derek E. Moulton, L. Angela Mihai, A rod theory for liquid crystalline elastomers, J. Elast. 153 (4–5) (2023) 509–532.

[9] Ethan S. Wold, Rundong Yang, James Lynch, Ellen Liu, Nick Gravish, Simon Sponberg, Supra-resonant wingbeats in insects, 2025, http://dx.doi.org/10.1101/2025.05.07.652680, BioRxiv, URL https://www.biorxiv.org/content/early/2025/05/11/2025.05.07.652680.

[10] R. Åke Norberg, Hovering flight of the dragonfly Aeschna juncea L., kinematics and aerodynamics, in: Swimming and Flying in Nature, vol. 2, Springer, 1975, pp. 763–781.

[11] Chris Somps, Marvin Luttges, Dragonfly flight: Novel uses of unsteady separated flows, Science 228 (4705) (1985) 1326–1329.

[12] J.M. Wakeling, C.P. Ellington, Dragonfly flight: II . Velocities, accelerations and kinematics of flapping flight, J. Exp. Biol. 200 (3) (1997) 557–582.

[13] Philip Hunter, The nature of flight: The molecules and mechanics of flight in animals, EMBO Rep. (ISSN: 1469-221X) 8 (9) (2007) 811–813, http://dx.doi.org/10.1038/sj.embor.7401050, (ISSN: 1469-3178).

[14] Lisa A. Treidel, Kevin D. Deem, Mary K. Salcedo, Michael H. Dickinson, Heather S. Bruce, Charles-A. Darveau, Bradley H. Dickerson, Olaf Ellers, Jordan R. Glass, Caleb M. Gordon, Jon F. Harrison, Tyson L. Hedrick, Meredith G. Johnson, Jacqueline E. Lebenzon, James H. Marden, Kristjan Niitepõld, Sanjay P. Sane, Simon Sponberg, Stav Talal, Caroline M Williams, Ethan S. Wold, Insect flight: State of the field and future directions, Integr. Comp. Biol. (ISSN: 1540-7063) 64 (2) (2024) 533–555, http://dx.doi.org/10.1093/icb/icae106, (ISSN: 1557-7023).

[15] Kevin Y. Ma, Pakpong Chirarattananon, Sawyer B. Fuller, Robert J. Wood, Controlled flight of a biologically inspired, insect-scale robot, Science (ISSN: 0036-8075) 340 (6132) (2013) 603–607, http://dx.doi.org/10.1126/science.1231806, (ISSN: 1095-9203).

[16] Owain Vaughan, RoboBee breaks free, Nat. Electron. (ISSN: 2520-1131) 2 (7) (2019) 265, http://dx.doi.org/10.1038/s41928-019-0280-8.

[17] Xiufeng Yang, Ying Chen, Longlong Chang, Ariel A. Calderon, Nestor O. Perez-Arancibia, Bee^{+} : A 95-Mg Four-Winged Insect-Scale Flying Robot Driven by Twinned Unimorph Actuators, IEEE Robot. Autom. Lett. (ISSN: 2377-3766) 4 (4) (2019) 4270–4277, http://dx.doi.org/10.1109/LRA.2019.2931177, (ISSN: 2377-3774).

[18] Ethan S. Wold, Brett Aiello, Manon Harris, Usama bin Sikandar, James Lynch, Nick Gravish, Simon Sponberg, Moth resonant mechanics are tuned to wingbeat frequency and energetic demands, Proc. R. Soc. B: Biol. Sci. (ISSN: 0962-8452) 291 (2025) (2024) 20240317, http://dx.doi.org/10.1098/rspb.2024.0317.

[19] Sophie Ramananarivo, Ramiro Godoy-Diana, Benjamin Thiria, Rather than resonance, flapping wing flyers may play on aerodynamics to improve performance, Proc. Natl. Acad. Sci. 108 (15) (2011) 5964–5969, http://dx.doi.org/10.1073/pnas.1017910108, URL https://www.pnas.org/doi/abs/10.1073/pnas.1017910108.

[20] Jeff Gau, James Lynch, Brett Aiello, Ethan Wold, Nick Gravish, Simon Sponberg, Bridging two insect flight modes in evolution, physiology and robophysics, Nature 622 (7984) (2023) 767–774, http://dx.doi.org/10.1038/s41586-023-06606-3.

[21] Robert K. Josephson, Jean G. Malamud, Darrell R. Stokes, Asynchronous muscle: A primer, J. Exp. Biol. (ISSN: 0022-0949) 203 (18) (2000) 2713–2722, http://dx.doi.org/10.1242/jeb.203.18.2713.

[22] Michael H. Dickinson, Fritz-Olaf Lehmann, Sanjay P. Sane, Wing rotation and the aerodynamic basis of insect flight, SCience 284 (5422) (1999) 1954–1960.

[23] Ali Hasan Nayfeh, Dean T. Mook, Nonlinear oscillations, in: Wiley Classics Library, John Wiley & Sons, Nashville, TN, 1995.

[24] Pauli Virtanen, Ralf Gommers, Travis E. Oliphant, Matt Haberland, Tyler Reddy, David Cournapeau, Evgeni Burovski, Pearu Peterson, Warren Weckesser, Jonathan Bright, et al., SciPy 1.0: Fundamental algorithms for scientific computing in Python, Nature Methods 17 (3) (2020) 261–272, http://dx.doi.org/10.1038/s41592-019-0686-2.